Carbohydrate Polymers 79 (2010) 1130–1139

Contents lists available at ScienceDirect

Carbohydrate Polymers

journal homepage: www.elsevier.com/locate/carbpol

Anti-thixotropic properties of waxy maize starch dispersions with different pasting conditions

Bao Wang [a], Dong Li [a,*], Li-Jun Wang [b], Necati Özkan [c]

[a] College of Engineering, China Agricultural University, P.O. Box 50, 17 Qinghua Donglu, Beijing 100083, China
[b] College of Food Science and Nutritional Engineering, China Agricultural University, Beijing, China
[c] Central Laboratory, Middle East Technical University, Ankara, Turkey

ARTICLE INFO

Article history:
Received 14 September 2009
Received in revised form 18 October 2009
Accepted 22 October 2009
Available online 25 October 2009

Keywords:
Rheological properties
Anti-thixotropy
Thixotropy
Waxy maize starch

ABSTRACT

The effects of pasting conditions, testing temperature, and shear rate on the anti-thixotropy of waxy maize starch (WMS) dispersions were investigated in this study. Activation energy and viscoelastic properties of the WMS dispersions were also determined to understand the anti-thixotropy of these dispersions. The WMS dispersions (5.0 wt.%) displayed both thixotropic and anti-thixotropic properties in loop and shear recovery tests, depending on pasting conditions and testing temperature. The standard anti-thixotropy test indicated anti-thixotropy of WMS dispersions only appeared at a certain shear rate range. When WMS dispersion was pasted more completely, the shear rate range for anti-thixotropy became wider, also the sample showed improved heat stability. The anti-thixotropy of the WMS dispersions was ascribed to re-range of the amylopectin molecules under appropriate shear rates. The normal maize starch (NMS) dispersion (5.0 wt.%) could not display anti-thixotropy here, due to a different paste structure formed by amylose in the continuous phase.

1. Introduction

Waxy maize starch (WMS), which contains about 99% amylopectin, is an essentially amylose-free starch (Achayuthakan & Suphantharika, 2008). Because of its unique composition, WMS has many specific attributes such as swelling easily, giving sticky texture, hardly retrograding, and better digestibility than normal starches (Enes, Panserat, Kaushik, & Oliva-Teles, 2006; Hibi, 2001), making it a promising raw material in food, medicine, and cosmetic industries (Lehmann, Volkert, Fischer, Schrader, & Nerenz, 2008; Sands, Leidy, Hamaker, Maguire, & Campbell, 2009; Wang et al., 2009a).

The rheological properties of starches are very important, which could determine their value and understand their behavior during the process. For example, in food technology, specific adjustment of the flow behavior of starch gels is significant in order to regulate production processes and to optimize applicability, stability, and sensory properties of the end products (Kulicke, Eidam, Kath, Kix, & Kull, 1996). In paper making and textile industries, the rheological properties of starch solutions could determine the loss of momentum during pipe transportation and the quality of final production. As a result, for a successful product formulation and engineering scale up, the knowledge about rheological properties of starch solutions is necessary (Bhandari, Singhal, & Kale, 2002).

In our last paper, the anti-thixotropic behavior of WMS dispersions was reported in the steady flow and in-shear structural recovery measurements (Wang et al., 2009a). Anti-thixotropy, which is also known as rheopexy (Dewar & Joyce, 2006), is just opposite to thixotropy of solutions or suspensions. It was reported that an anti-thixotropic behavior is observed when viscosity increases with time at a fixed shear rate, while a thixotropic effect is described as a viscosity decrease with time at a constant shear rate (Gouveia, Muller, Marchal, & Choplin, 2008). Besides, the anti-thixotropic properties could also be determined through a steady shear tests involving a rate ramp up to a peak shear rate, then a ramp down back to zero; and the fluids with such properties could display an anti-hysteresis in the form of a counterclockwise loop (Achayuthakan & Suphantharika, 2008; Acquarone & Rao, 2003; Tattiyakul & Rao, 2000; Wang et al., 2009a). Anti-thixotropy of liquids or suspensions has important significance in industries, such as cement with rheopectic property which can be used in building a bridge pier underwater, or molding plaster with anti-thixotropic behavior, which could accelerate solidification and molding under shaking.

Till now, only limited messages were given about the anti-thixotropy of starch dispersions. In our last study, it was found that the anti-thixotropy of WMS dispersions had some relationships with pasting conditions. It seems WMS dispersions only displayed such

* Corresponding author. Tel./fax: +86 10 62737351.
E-mail address: dongli@cau.edu.cn (D. Li).

0144-8617/$ - see front matter © 2009 Elsevier Ltd. All rights reserved.
doi:10.1016/j.carbpol.2009.10.053

Nomenclature

E_a	activation energy (J/mol)	R	gas constant (J/mol K)
G'	storage modulus (Pa)	R^2	correlation coefficient (dimensionless)
G''	loss modulus (Pa)	T	absolute temperature (K)
K'	index (Pa s^n)	$\dot{\gamma}$	shear rate (s^{-1})
K''	index (Pa s^n)	η_a	apparent viscosity (Pa s)
n'	frequency exponent (dimensionless)	η_∞	frequency factor (dimensionless)
n''	frequency exponent (dimensionless)	ω	angular frequency (rad/s)

properties after being sufficiently pasted (Wang et al., 2009a). Since there are still many questions about this problem, the anti-thixotropy of WMS dispersions was further investigated in this study, which will help to provide useful messages for the industrial production of the WMS based foods.

During the study, the effects of several factors (such as pasting conditions, testing temperature, shear rate, etc.) on the anti-thixotropy were investigated. In previous reports, the anti-thixotropy of starch dispersions was mainly reported of waxy starches or modified waxy starches (Tattiyakul & Rao, 2000). Therefore, in order to determine whether such a behavior was unique to waxy starch, normal maize starch (NMS) was also used as a reference. Besides, the effect of temperature on apparent viscosity, viscoelastic properties, and micro-structure of the samples were also studied to understand the anti-thixotropy of starch dispersions.

2. Materials and methods

2.1. Materials

Commercial WMS (10.04 wt.% moisture (wet basis) and trace amount of amylose) was purchased from Jinan Jinwang Food Co., Ltd. (Shandong Province, China). Commercial NMS (12.43 wt.% moisture (wet basis) and 22% amylose) was purchased from Weizhiyuan Food Co., Ltd. (Beijing, China).

2.2. Preparation of WMS and NWS dispersions with different pasting conditions

WMS suspension (5.0 wt.%) was prepared by adding 7.5 g WMS into 142.5 g deionized water at room temperature (about 25 °C). Three different pasting methods were adopted to study the effect of pasting conditions on the rheological properties of WMS dispersions (A): Well mixed WMS suspension (150 g) in conical flask was heated in a water bath at 95 °C for 6 min with a constant mixing rate of 200 rpm controlled by a digital mixer (EUROSTAR, IKA Instruments, Germany). (B): Well mixed WMS suspension (150 g) was heated in a water bath at 95 °C for 40 min with a constant mixing rate of 200 rpm. (C): Well mixed WMS suspension (150 g) was heated in a water bath at 95 °C for 40 min with a constant mixing rate of 400 rpm. (D): As a reference, well mixed NMS suspension (150 g, 5.0 wt.%) was pasted with the same procedure as (C). Then the dispersions from (A)–(C) were rapidly cooled in another water bath, and stored in an incubator (GP-01, Hubei Province, China) at 25 °C for 2 h before testing. After pasting, the dispersion of NMS was rapidly cooled in another water bath, and then stored in the incubator at 40 °C for 2 h before measurements. The storage temperature of 40 °C was chosen in order to prevent gel formation of NMS dispersion (Pongsawatmanit, Temsiripong, & Suwonsichon, 2007). The dispersions pasted from procedures (A)–(D) were signed as the dispersions A–D, respectively.

2.3. Rheological tests

Rheological properties of all samples were measured using AR2000ex rheometer (TA Instruments Ltd., Crawley, UK) with aluminum parallel plate geometry (40 mm diameter, 1 mm gap). The temperature was controlled by a water bath connected to the Peltier system in the bottom plate. A thin layer of silicone oil was applied on the surface of the samples in order to prevent evaporation. For each sample, steady flow tests, in-shear structural recovery, standard anti-thixotropy, effect of temperature on apparent viscosity, and viscoelastic properties were determined.

2.3.1. Steady flow measurements

Steady flow measurements were performed at 25 °C, 50 °C and 75 °C to obtain shear rate versus shear stress data. The sample was placed in the rheometer and pre-sheared at 100 s^{-1} for 30 s, and then it was equilibrated at the testing temperatures for 5 min before measurement. The shear rate was programmed to increase from 0 to 300 s^{-1} in 3 min, then followed immediately by a reduction from 300 to 0 s^{-1} in the next 3 min.

2.3.2. In-shear structural recovery measurements

In-shear structural recovery of the samples was determined according to the procedure of Mezger (2002) with some modifications. The sample was loaded into the rheometer and pre-sheared at 100 s^{-1} for 30 s, and subsequently it was equilibrated at the testing temperature (i.e. 25, 50 and 75 °C) for 5 min before measurement. A three stepped shear flow test was performed as follows: (1) a constant shear rate of 1 s^{-1} was applied for 120 s and subsequently (2) a constant shear rate of 300 s^{-1} was applied for 60 s, and then (3) a constant shear rate of 1 s^{-1} was applied for 180 s. The in-shear recovery value was calculated as the ratio of average apparent viscosity (η_a) obtained during the first 120 s of the third step to the average η_a value determined in the first step.

2.3.3. Standard anti-thixotropy test

The definition of anti-thixotropy is an increase in apparent viscosity with time under constant shear rate (Ferguson & Kembowski, 1995; Gouveia et al., 2008). In this test, the samples were sheared at a fixed shear rate (1, 10, 50, 100 s^{-1}, etc.) for a specific amount of time (10 min 30 s), and the viscosity was recorded in order to determine the anti-thixotropic behavior of the samples.

2.3.4. Effect of temperature on apparent viscosity

The sample was loaded into the rheometer and equilibrated at the testing temperature (5, 15, 25, 35 and 45 °C, respectively) for 5 min before measurement, and then the apparent viscosity ($\eta_{a,10}$) was determined as the average value of the first two minutes at a constant shear rate of 10 s^{-1}. Arrhenius equation was used to determine the activation energy (E_a) and to investigate the temperature dependency of the apparent viscosity of all samples (Pongsawatmanit, Temsiripong, Ikeda, & Nishinari, 2006; Wang, Wang, Li, Xue, & Mao, 2009b). The effect of temperature

on η_a of the dispersions was studied using the Arrhenius equation (Eq. (1)).

$$\eta_{a,10} = \eta_\infty \exp(E_a/RT) \quad (1)$$

where $\eta_{a,10}$ is the apparent viscosity (Pa s) at 10 s^{-1}, η_∞ is the frequency factor, E_a is the activation energy (J/mol), R is the gas constant (8.3145 J/mol K), and T is the absolute temperature (K).

2.3.5. Viscoelastic properties

Small amplitude oscillatory tests were performed at 25 °C over the frequency range of 0.1–10 Hz (0.628–62.8 rad/s). Before measurement, the sample was loaded into the rheometer and rested for 3 min. The strain amplitude for the frequency sweep measurements was selected as 1%, which was in the linear viscoelastic region for all samples. The mechanical spectra were obtained recording storage modulus (G'), loss modulus (G'') and loss tangent ($\tan\ \delta = G''/G'$) as a function of angular frequency (ω).

2.4. Microscopy study

In order to investigate the relationship between rheological properties and microscopic structures of the dispersions, all samples were observed using an optical microscope (CX31 Biological Microscope, Olympus Corporation, Japan) equipped with a CCD camera module.

2.5. Statistical analysis

All experiments described above were made in triplicate for each sample. The data presented were the means and standard deviations of each experiment. A one-way analysis of variance (ANOVA) and Tukey's test were used to establish the significance of differences among the mean values at the 0.95 level of confidence. The statistical analysis was performed using SPSS (2003) version 13.0 for Windows program (SPSS Inc., Chicage, IL, USA).

3. Results and discussion

3.1. Steady flow measurements

As indicated by previous report, temperature during distribution and storage before consumption is an important environmental factor which could determine the final stability of the required texture attributes of starch dispersions, so the study of temperature on rheological properties of starch dispersions will help to predict and control the change of physical properties of starch-based foods (Pongsawatmanit et al., 2006). As indicated in Fig. 1, the flow curves of all samples were affected by temperature obviously. Generally, lower apparent viscosity (η_a) could be observed at higher temperatures for the same sample. It is accepted that η_a of a liquid is a function of the intermolecular forces that restrict molecular motion (Nurul, Azemi, & Manan, 1999). When the temperature was higher, there was an increase in kinetic energy of the dispersions, thus the polysaccharide molecules became more flexible which could help to the disentanglement of long chain molecules, as a result the viscosity of dispersions was reduced.

As can be seen from Fig. 1(A), the dispersion A displayed clockwise hysteresis loops at all testing temperatures, suggesting that this sample showed thixotropic behavior (Acquarone & Rao, 2003). It was observed that the area of the hysteresis loop became much smaller at 50 °C and 75 °C compared to 25 °C, which indicated a relatively smaller damage of the paste structure at higher temperature during the increasing-order of shear rate (up curve). The dispersion B (see Fig. 1(B)) at 25 °C was characterized by a combined hysteresis loop, i.e., a big clockwise loop at high shear rates (50–300 s^{-1}) and a relatively small counterclockwise loop at low shear rates (0–50 s^{-1}). When tested at 50 °C, the anticlockwise loop (0–100 s^{-1}) became bigger in relation to the clockwise loop (100–200 s^{-1}). At 75 °C, the clockwise loop of the dispersion B almost disappeared, indicating no hysteresis appeared at high shear rates; meanwhile, the counterclockwise loop at low shear rates grew bigger than the one at 50 °C, which suggested an anti-thixotropic behavior (Acquarone & Rao, 2003; Wang et al., 2009a). Similar flow curves as shown in Fig. 1(B) were reported by Tattiyakul and Rao (2000). The flow curve of the dispersion C at 25 °C (Fig. 1(C)) showed a weak clockwise loop at high shear rates (150–300 s^{-1}) compared with the counterclockwise loop at low shear rates (0–150 s^{-1}). At 50 °C and 75 °C, the clockwise loop disappeared completely, and the dispersion C displayed distinct counterclockwise loop over the whole shear rate range, indicating an obvious anti-thixotropic behavior. Such results suggested that new structures of the dispersion C, which were more stable and resistant to shearing, could be formed during the up curve at 50 °C and 75 °C, suggesting that the formation of the new structures accelerated at higher temperatures (50 °C and 75 °C).

From the dispersions A–C, it could be concluded that both heating time and mixing rate during pasting could affect the rheological properties of WMS dispersions. For example, with the same mixing rate (200 rpm), dispersion B with longer heating time (40 min) displayed thixotropic behavior at 25 °C and weak anti-thixotropic behavior at 50 and 75 °C, while dispersion A with shorter heating time (6 min) could only display thixotropic property at all the testing temperatures, as can be seen in Fig. 1(A) and (B). Similarly, with the same heating time (40 min), higher mixing rate made dispersion C (400 rpm) display a more distinct anti-thixotropic behavior than dispersion B (200 rpm), as shown in Fig. 1(B) and (C). Obviously, longer heating time and higher mixing rate during pasting could break the starch granules more thoroughly, and make the dispersion pasted more completely. In general, the WMS dispersion which pasted more completely with more granules dissolved into the continuous phase could display a more obvious anti-thixotropic behavior under the same testing conditions. Such results suggested the anti-thixotropy of WMS dispersion should be ascribed to amylopectin dissolved in the continuous phase, in agreement with previous studies (Wang et al., 2009a). When the WMS dispersion was pasted severely, the starch granules were destroyed and more amylopectin dissolved into the continuous phase, as a result, the anti-thixotropy behavior of the dispersions were enhanced under shearing.

The effect of temperature on the flow curves of the dispersions A–C also illuminated the decisive effect of amylopectin molecules on the anti-thixotropic behavior. Generally speaking, when the test temperature increased from 25 °C to 50 °C and 75 °C, the amylopectin in the continuous phase became more active, thus a more obvious anti-thixotropic behavior for the dispersions was observed. As for the dispersion B, the shapes of its flow curves changed from a clockwise loop to a combined loop and then to a counterclockwise loop with the increase of temperature, suggesting that the thixotropy of the dispersion B at 25 °C developed into anti-thixotropy with the increase of temperature. On the other hand, the effect of temperature on anti-thixotropic behavior also suggested such a behavior was not due to the formation of granule clusters during shearing as suggested by Chamberlain, Rao, and Cohen (1999), for the motion of the starch granules was not obviously affected by the temperature increase here.

It might be assumed that the anti-thixotropy of WMS dispersions under shearing was due to the formation of more bonds between the amylopectin molecules, which facilitated the formation of a more complex structure of the dispersions. Similar explanation could be found by previous investigation (Dewar & Joyce, 2006). In

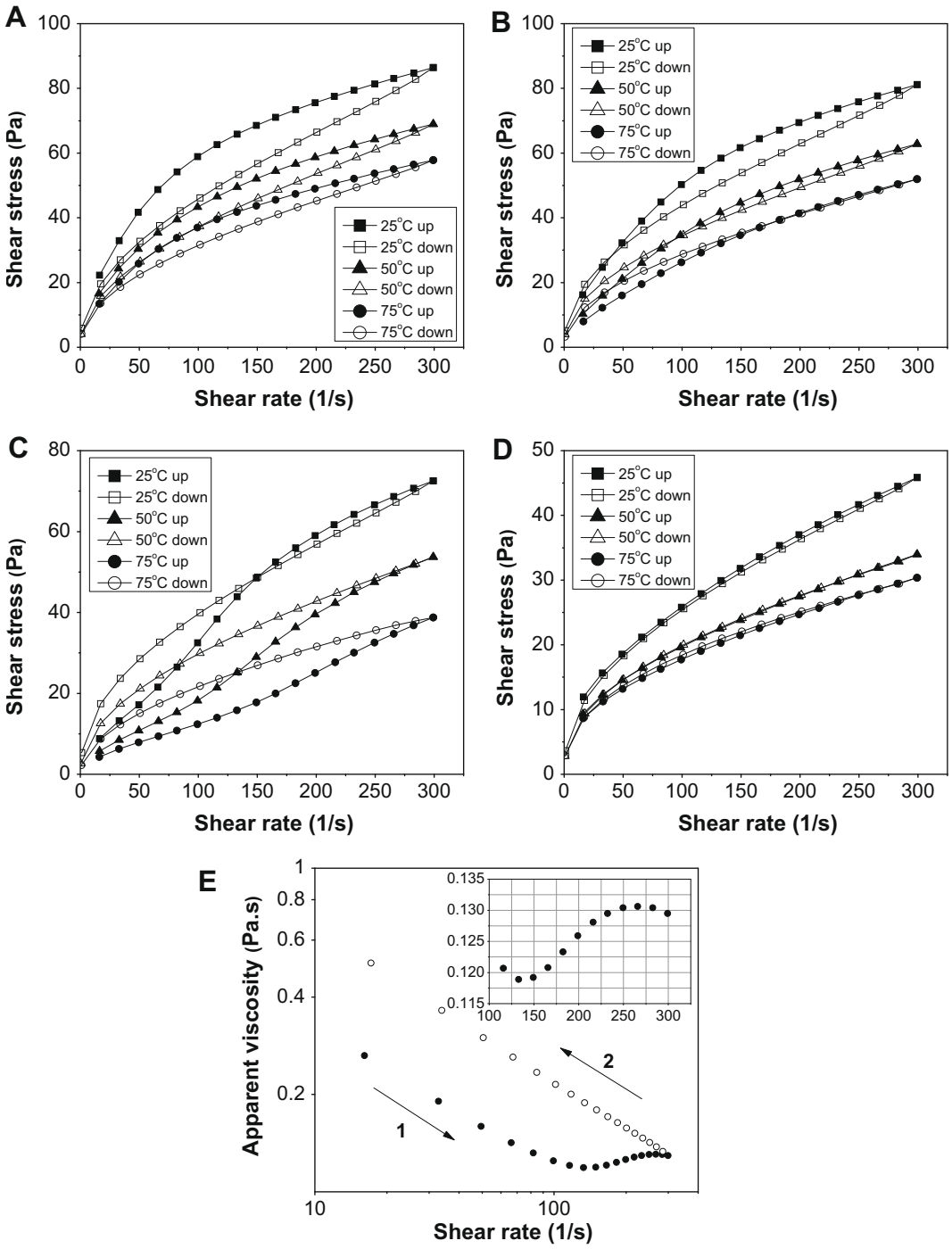

Fig. 1. Flow curves of the samples: (A) WMS (5.0 wt.%) pasted for 6 min, 200 rpm; (B) WMS (5.0 wt.%) pasted for 40 min, 200 rpm; (C) WMS (5.0 wt.%) pasted for 40 min, 400 rpm; (D) NMS (5.0 wt.%) pasted for 40 min, 400 rpm; and (E) apparent viscosity against shear rate for the sample C.

the report of Dewar and Joyce (2006), the maize starch based thickener (99.2% maize starch, 0.4% sucrose, 0.3% glucose, 0.1% lactose) at the concentrations of 4 and 5% displayed a anti-thixotropic behavior. They suggested that the densely packed samples were restricted in movement, and only some bonds could be formed by Brownian motion. So when the dispersions were sheared, the molecules were allowed to make more collisions and more permutations of molecular orientations during collisions, which formed more bonds and created a more complex three-dimensional structure, meaning that shearing these dispersions resulted in the increasing of apparent viscosity. However, it was not clear whether the maize starch in their study was WMS or not.

Even though the dispersion D (Fig. 1(D)) was sufficiently pasted (with the same pasting procedure of the dispersion C), no obvious hysteresis loop was found from its flow curves, suggesting that no structural re-organization took place during shearing. This observation indicated that only the WMS dispersions pasted sufficiently could display the anti-thixotropic behavior. During the pasting of the NMS dispersion, the amylose might have been leached out from the granules (Iturriage, Mishima, & Anon, 2006); as a result

the paste structure of the NMS dispersions was changed, resulting in different rheological properties.

Besides, it was found in this study that the dispersion C could display shear-thickening behavior at certain shear rate range. Shear thickening, which can be defined as the increasing of the apparent viscosity with the increasing of shear rate or applied stress, was different from the definition of anti-thixotropy. Fig. 1(E) shows the apparent viscosity of the dispersion C as a function of shear rate at 75 °C. From Fig. 1(E), it could be observed that the dispersion C displayed a distinct shear-thickening behavior during the increasing-order of shear rate ranging from about 150 to 275 s^{-1}, however, the shear-thickening behavior for this dispersion was not observed during the decreasing-order of shear rate. Similar results were reported for a WMS solution (2% in NaOH solution medium (1 mol/L)), and the shear-thickening behavior was attributed to increase of the effective starch concentration, caused by the breaking up of the gel-like starch clusters which was macroscopically heterogeneous (Kim, Willett, Carriere, & Felker, 2002). However, more investigations need to be carried because the preparation methods in this study were quite different from Kim et al. (2002).

3.2. In-shear structural recovery measurements

Even though the loop test described in Section 3.1 is quick and qualitative, it has certain limitations. One limitation of the test is that both shear rate and time are changed simultaneously, which cannot be resolved into the separate effects of these two parameters (Barnes, 1997; Mewis & Wagner, 2009). Furthermore, hysteresis is not unique to thixotropic materials, which also occurs in the case of irreversible work softening and in viscoelastic materials (Bird & Marsh, 1968). Thus, a simpler and more quantitative test can be performed using step-wise changes in shear rate, where the shear rate is changed from one constant value to another with a carefully controlled prehistory, such as the shear recovery test (Barnes, 1997; Dewar & Joyce, 2006).

The in-shear structural recovery test can be used to investigate the capability of the dispersions to recover their original structure under low shear conditions after decomposition under high-shear conditions (Mezger, 2002). The viscosity profiles as a function of time for the starch dispersions are given in Fig. 2.

As can be seen from Fig. 2, the apparent viscosity of the dispersion A at the same temperature was the highest followed by these of the dispersions B and C, suggesting that when the extent of pasting was increased, the apparent viscosity of the dispersions was decreased. The influence of temperature on the apparent viscosity of the starch dispersions can also be seen in Fig. 2. For the first step of shearing, the apparent viscosity of all starch samples was decreased with the increasing of temperature from 25 °C to 75 °C. For the third step, the apparent viscosity of the samples A–C changed proportionally as a function of temperature, however, a similar behavior was not observed for the sample D. It was reported that in the step-wise change of shear rate, when the shear rate was suddenly stepped up or down, the subsequent viscosity transients could reflect the changes in micro-structure under well-defined flow conditions (Mewis & Wagner, 2009). Therefore, such results may suggest the differences of micro-structures between the pastes of WMS and NMS.

The quantitative results of the in-shear structural recovery test for the starch dispersions were given in Table 1. From Table 1, both the pasting conditions and testing temperature could affect the recovery values of the WMS dispersions. In this study, generally a more complete pasting with longer heating time and higher mixing rate of the WMS dispersion could bring a higher recovery value, suggesting the recovery value was determined by the continuous phase of the WMS dispersions. Such a change trend of recovery values also indicated that longer heating time and higher mixing rate during pasting could break the starch granules more thoroughly, make the dispersion pasted more completely, and consequently change the rheological properties of the WMS dispersions, as indicated in Section 3.1. For the dispersion A at 25 °C, the recovery value was 0.93 ± 0.01, suggesting that the original structure of the dispersion A was destroyed, while the new structure formed later was slightly less resistant to shearing. Perhaps the highly solvated granules in the structure of sample A (see Fig. 6(A)) were sheared into smaller fragments under high-rate shearing conditions (Wang et al., 2008), which then decreased the resistance to shearing after the high-shear step. For the testing of 50 °C and 75 °C, the recovery value for the dispersion A was larger than 1 (1.18 ± 0.01 and 1.24 ± 0.03, respectively), indicating a greater effect of amylopectin in the continuous phase, which was more flexible at higher temperatures and could conduce to the formation of more stable structure during high-rate shearing. The recovery value of the dispersion B increased from 1.41 ± 0.01 (25 °C) to 1.83 ± 0.05 (50 °C) and 1.90 ± 0.09 (75 °C) with increasing of temperature, suggesting a stronger anti-thixotropic behavior could bring a higher recover value, in accordance with the change from thixotropy to anti-thixotropy with temperature increase as shown in Fig. 1(B). Since the dispersion C was most completely pasted, its recovery value was larger than other samples at the same temperature. However, when temperature increased from 50 °C to 75 °C, the recovery value decreased from 3.14 ± 0.04 to 2.59 ± 0.03, indicating shear recovery was not a simple function of temperature. Since the amylopectin molecules of the dispersion C in the continuous phase were most flexible and vulnerable to temperature than other samples, thus when temperature was higher than a critical value, the decrease of η_a may dominate the third step, resulting a smaller recovery value.

For the NMS dispersions (Fig. 2(D)), the recovery values were 0.84 ± 0.01 (25 °C), 0.97 ± 0.01 (50 °C) and 1.01 ± 0.02 (75 °C), respectively. Even the dispersion D was sufficiently pasted, the recovery value for the dispersion D at 75 °C was not significantly larger than 1, indicating new structure which was more shear-resistant could not formed during high-rate shearing. With almost all the granules dissolved into the continuous phase (Section 3.5), the dispersion D was assumed to display a stronger liquid-like behavior at higher temperature, which caused the increase of the recovery value.

3.3. Standard anti-thixotropy test

As indicated above, the definition of anti-thixotropy is an increase in apparent viscosity with time under constant shear rate, while a thixotropic effect is described as a viscosity decrease with time at a constant shear rate (Ferguson & Kembowski, 1995; Gouveia et al., 2008). Therefore, the (anti-)thixotropy of the samples could be determined in a direct way through the viscosity test under fixed shear rate.

From Fig. 3(A), the viscosity of the dispersion A increased gradually and then reached a equilibrium at the shear rate ($\dot{\gamma}$) of 1 s^{-1}, which indicated the anti-thixotropy of the dispersion A at this shear rate. When $\dot{\gamma}$ was set at 10 s^{-1}, the viscosity curve increased during the first 60 s, then decreased gradually. When the shear rate became higher (50, 100 and 150 s^{-1}), the viscosity curve displayed thixotropic behavior, which decreased along with time. For the dispersion B (Fig. 3(B)), the viscosity curve of 1 s^{-1} was quite steady. When $\dot{\gamma}$ was set at 10 s^{-1}, the flow curve of the dispersion B displayed significant anti-thixotropic property, which increased continuously until the end of the test. The anti-thixotropy of the dispersion B became weak and turned into thixotropic behavior at higher shear rates (50, 100, 150 s^{-1}). The dispersion C (Fig. 3(C)) displayed distinct anti-thixotropy at the shear rates of

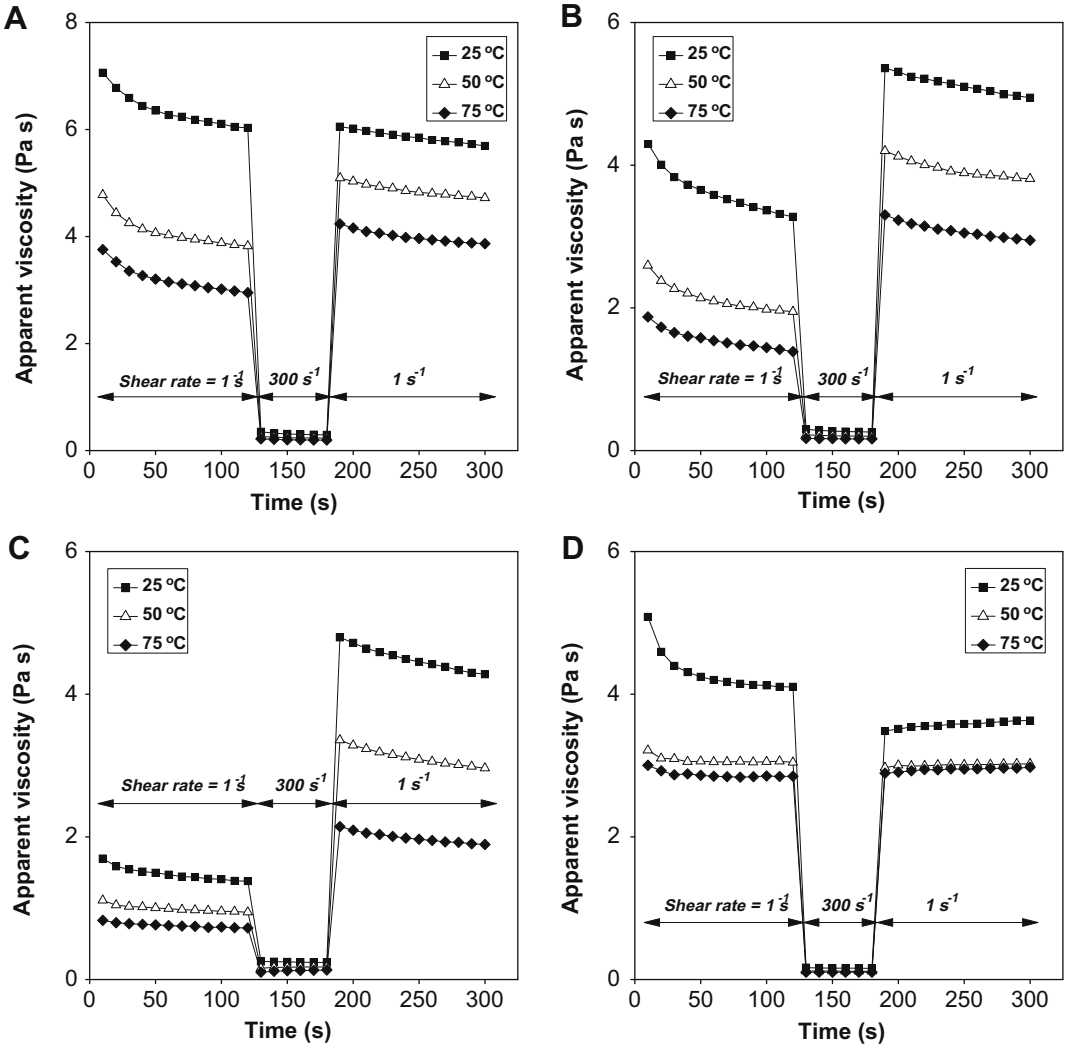

Fig. 2. In-shear structural recovery of the samples determined at 25, 50 and 75 °C: (A) WMS (5.0 wt.%) pasted for 6 min, 200 rpm; (B) WMS (5.0 wt.%) pasted for 40 min, 200 rpm; (C) WMS (5.0 wt.%) pasted for 40 min, 400 rpm; and (D) NMS (5.0 wt.%) pasted for 40 min, 400 rpm.

Table 1
In-shear recovery properties of the samples determined at 25, 50 and 75 °C.[a,b]

Samples	Temperature (°C)	Step 1 (Pa s)	Step 2 (Pa s)	Step 3 (Pa s)	Recovery step 3/step 1
A	25	6.27 ± 0.09[a]	0.31 ± 0.00[a]	5.81 ± 0.06[a]	0.93 ± 0.01[a]
	50	4.16 ± 0.13[b]	0.24 ± 0.00[b]	4.90 ± 0.09[b]	1.18 ± 0.01[b]
	75	3.25 ± 0.12[c]	0.20 ± 0.00[c]	4.04 ± 0.04[c]	1.24 ± 0.03[c]
B	25	3.57 ± 0.09[a]	0.27 ± 0.00[a]	5.04 ± 0.12[a]	1.41 ± 0.01[a]
	50	2.19 ± 0.08[b]	0.21 ± 0.00[b]	3.99 ± 0.04[b]	1.83 ± 0.05[b]
	75	1.66 ± 0.10[c]	0.17 ± 0.00[c]	3.14 ± 0.05[c]	1.90 ± 0.09[b]
C	25	1.49 ± 0.01[a]	0.24 ± 0.00[a]	4.50 ± 0.00[a]	3.03 ± 0.02[a]
	50	0.98 ± 0.03[b]	0.17 ± 0.00[b]	3.09 ± 0.05[b]	3.14 ± 0.04[b]
	75	0.75 ± 0.02[c]	0.12 ± 0.00[c]	1.95 ± 0.04[c]	2.59 ± 0.03[c]
D	25	4.28 ± 0.13[a]	0.16 ± 0.00[a]	3.57 ± 0.12[a]	0.84 ± 0.01[a]
	50	3.09 ± 0.03[b]	0.12 ± 0.00[b]	3.01 ± 0.04[b]	0.97 ± 0.01[b]
	75	2.92 ± 0.04[b]	0.10 ± 0.00[c]	2.96 ± 0.06[b]	1.01 ± 0.02[c]

[a] (A) WMS (5.0 wt.%) pasted for 6 min, 200 rpm; (B) WMS (5.0 wt.%) pasted for 40 min, 200 rpm; (C) WMS (5.0 wt.%) pasted for 40 min, 400 rpm; and (D) NMS (5.0 wt.%) pasted for 40 min, 400 rpm. The program in this test was: step 1, shear rate at 1 s^{-1} for 120 s; step 2, shear rate at 300 s^{-1} for 60 s; step 3, shear rate at 1 s^{-1} for 180 s.
[b] Assays were performed in triplicate at 25 °C. Mean ± standard deviation values in the same column for each solution followed by different superscripts are significantly different ($p \leqslant 0.05$).

10 and 50 s^{-1}, which increased continuously during the test. When $\dot{\gamma}$ was set at 100 and 150 s^{-1}, equilibrium could be reached after the initial increase of viscosity. When the shear rate was increased further (200, 300, and 400 s^{-1}), the dispersion C mainly displayed thixotropic property. As can be seen from Fig. 3(A–C), the anti-thixotropy of WMS dispersions only appeared at a certain shear rate

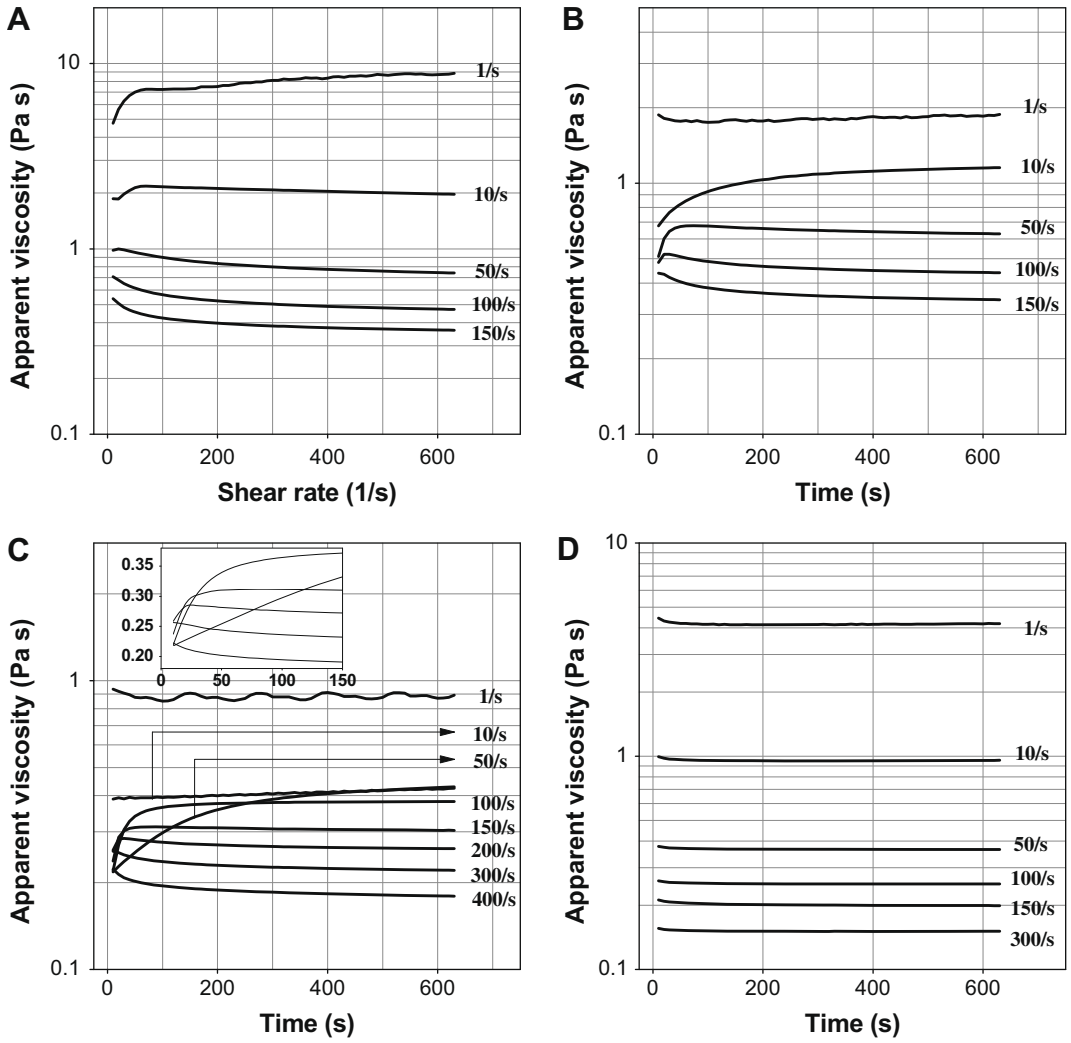

Fig. 3. Apparent viscosity of the samples under constant shear rate: (A) WMS (5.0 wt.%) pasted for 6 min, 200 rpm; (B) WMS (5.0 wt.%) pasted for 40 min, 200 rpm; (C) WMS (5.0 wt.%) pasted for 40 min, 400 rpm; and (D) NMS (5.0 wt.%) pasted for 40 min, 400 rpm.

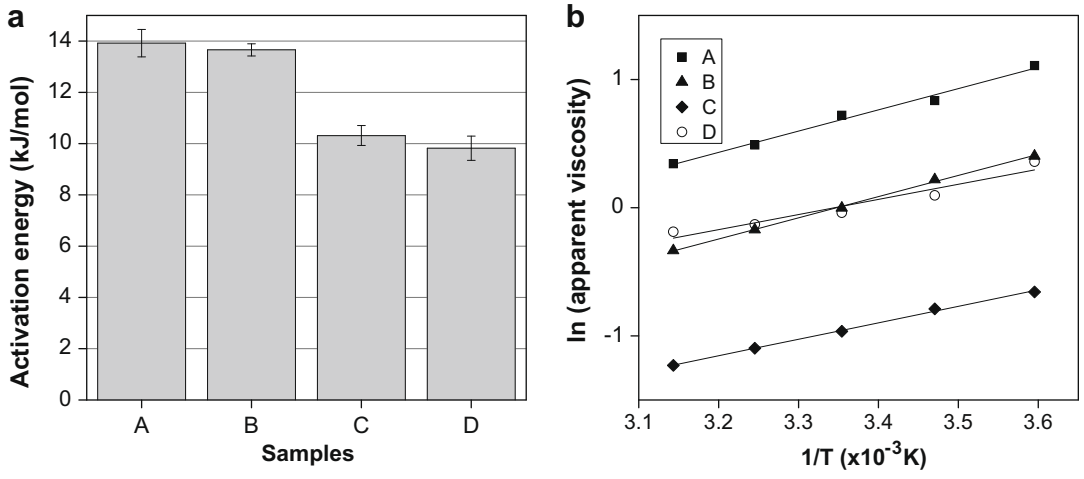

Fig. 4. Activation energy (a) and Arrhenius plots for apparent viscosity at a fixed shear rate of 10 s^{-1} (b) of the samples: (A) WMS (5.0 wt.%) pasted for 6 min, 200 rpm; (B) WMS (5.0 wt.%) pasted for 40 min, 200 rpm; (C) WMS (5.0 wt.%) pasted for 40 min, 400 rpm; and (D) NMS (5.0 wt.%) pasted for 40 min, 400 rpm.

range; when the dispersions were more completely pasted, such a property could be displayed at higher shear rates and wider shear rate range.

The similar types of anti-thixotropic behavior were reported for hydrophobically modified polyacrylamides aqueous solutions with sodium dodecyl sulfate during the step shear rate experiments, and

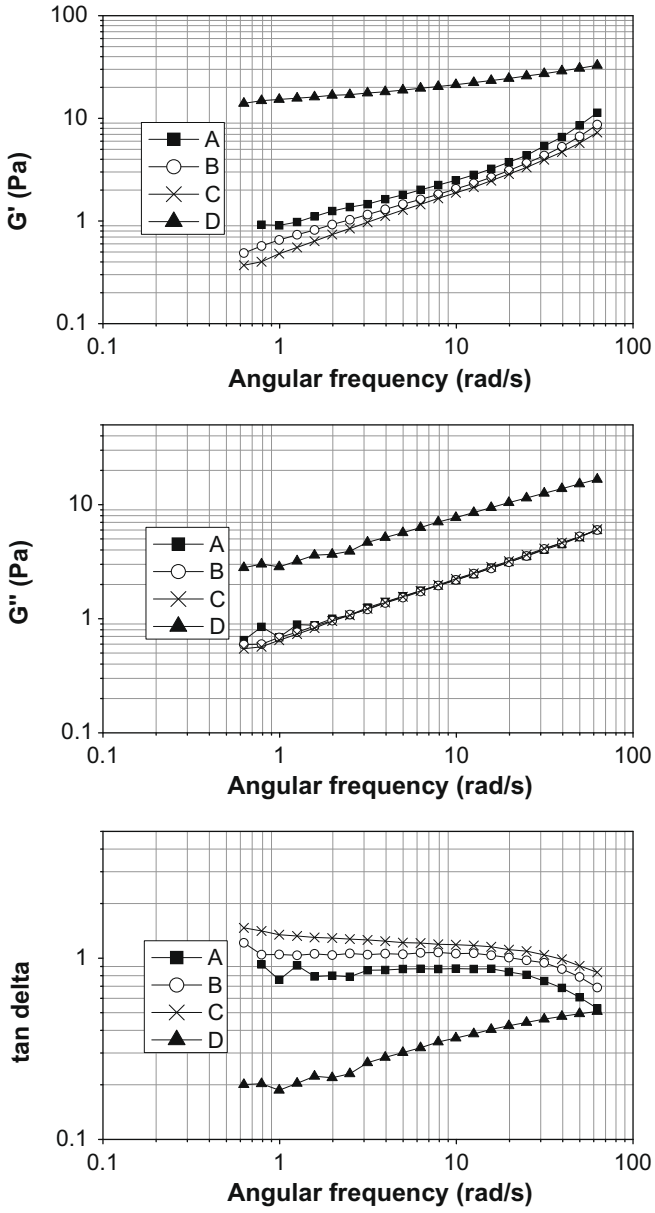

Fig. 5. Frequency dependence of G', G'' and tan δ of the samples determined at 25 °C: (A) WMS (5.0 wt.%) pasted for 6 min, 200 rpm; (B) WMS (5.0 wt.%) pasted for 40 min, 200 rpm; (C) WMS (5.0 wt.%) pasted for 40 min, 400 rpm; and (D) NMS (5.0 wt.%) pasted for 40 min, 400 rpm.

the viscosity increase over time was attributed to bridging of two or more polymer chains (Gouveia et al., 2008). In this study, the anti-thixotropy of the WMS dispersion could be ascribed to the interaction between the amylopectin molecules and formation of the new structure, as indicated above.

For the dispersion D, the flow curves kept almost constant at all the shear rates, proving that there was no change of the microstructure of the pastes during shearing, which was in accordance with the Sections 3.1 and 3.2. Such results also suggested anti-thixotropic behavior was unique to WMS dispersions in this study.

3.4. Effect of temperature on apparent viscosity

The activation energy (E_a), which was determined by an Arrhenius model (Eq. (1)), is a parameter reflecting the sensitivity of the apparent viscosity (η_a) change due to the temperature change (Blanshard, 1995; Rao, 1995). Starch-based products are generally processed and stored in a wide temperature range, so the study of the effects of temperature on the viscosity of starch dispersions is very important (Kim & Yoo, 2009). Also, this study could help to give a comprehensive understanding of the anti-thixotropy, which was obviously affected by temperature.

The E_a values and the Arrhenius plots of the starch dispersions are displayed in Fig. 4(a) and (b), respectively. From Fig. 4(a), when the WMS pasted more completely, there will be a smaller temperature dependence of the $\eta_{a,10}$ indicated by lower E_a. The E_a value of the dispersion B was smaller than that of the dispersion A, but the difference was weak and not significant ($p > 0.05$, data not shown). The E_a value of the dispersion C was significantly smaller than those of the dispersions A and B, suggesting that the heat stability of the WMS dispersions was improved after being subject to a more complete pasting. As indicated in Table 1, the difference between the recovery values of the dispersion C at 25 °C and 50 °C was relatively smaller than the corresponding values of the dispersions A and B, which might be ascribed to a better heat stability of the dispersion C as indicated here.

It was also reported that a lower activation energy for flowing indicated fewer inter- and intra-interactions between polysaccharide chains at the concentration studied (Mohammadifar, Musavi, Kiumarsi, & Williams, 2006), suggesting that the dispersion C, which displayed anti-thixotropic behavior, had less interactions between its molecules compared to the dispersions A and B. It should be pointed out that the anti-thixotropic behavior of the WMS dispersions was not directly relevant to the interaction level between the amylopectin molecules, and only under appropriate interaction level between the polysaccharide chains (i.e. at appropriate shear rates) could the WMS dispersion display the anti-thixotropic property, as indicated in Section 3.3.

The E_a value of the dispersion D was smaller than that of the dispersions A–C, as shown in Fig. 4, indicating that the dispersion D had the best heat stability within all samples. Even with the same pasting procedure, the viscosity value of the dispersion D was obviously higher than that of the dispersion C (Fig. 4(b)),

Table 2
Variation of G', G'', and tan δ with angular frequency for the samples determined at 25 °C.[a,b]

Sample	G'			G''		
	K'	n'	R^2	K''	n''	R^2
A	0.86 ± 0.04[a]	0.54 ± 0.02[a]	0.962	0.77 ± 0.01[a]	0.48 ± 0.00[a]	0.985
B	0.62 ± 0.02[b]	0.55 ± 0.03[a]	0.990	0.67 ± 0.01[b]	0.52 ± 0.01[b]	0.999
C	0.48 ± 0.01[b]	0.63 ± 0.02[b]	0.997	0.67 ± 0.02[b]	0.53 ± 0.00[b]	1.000
D	14.76 ± 0.16[c]	0.17 ± 0.01[c]	0.985	3.03 ± 0.04[c]	0.41 ± 0.00[c]	0.995

[a] (A) WMS (5.0 wt.%) pasted for 6 min, 200 rpm; (B) WMS (5.0 wt.%) pasted for 40 min, 200 rpm; (C) WMS (5.0 wt.%) pasted for 40 min, 400 rpm; and (D) NMS (5.0 wt.%) pasted for 40 min, 400 rpm.

[b] Assays were performed in triplicate at 1% strain. Mean ± standard deviation values in the same column for each solution followed by different superscripts are significantly different ($p \leqslant 0.05$).

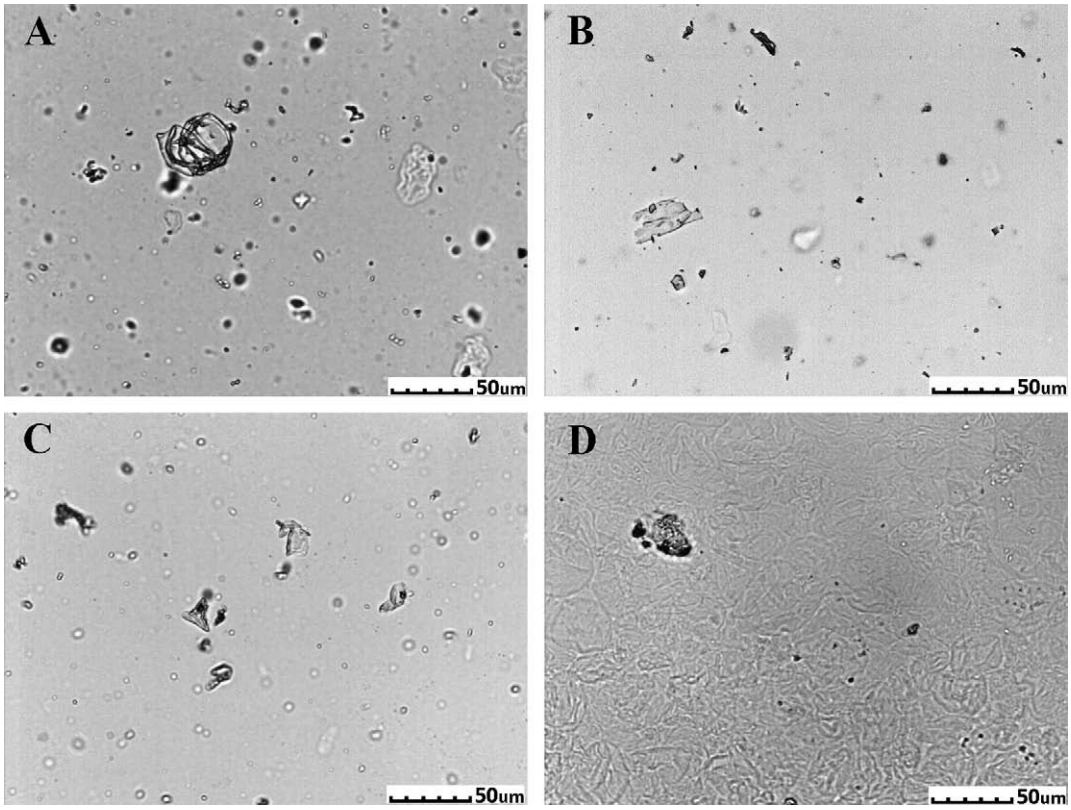

Fig. 6. Micrographs of the samples: (A) WMS (5.0 wt.%) pasted for 6 min, 200 rpm; (B) WMS (5.0 wt.%) pasted for 40 min, 200 rpm; (C) WMS (5.0 wt.%) pasted for 40 min, 400 rpm; and (D) NMS (5.0 wt.%) pasted for 40 min, 400 rpm.

which should be ascribed to amylose molecules leached out from the NMS granules during pasting. It is reported that amylose molecules in the continuous phase of normal starch dispersions have the capacity to form a network stabilized by hydrogen bonds (Iturriage et al., 2006), as a result, the viscosity of the dispersion D was higher than that of the dispersion C. At 5 °C, the amylose in the continuous phase of the pastes formed the gel-type structures quickly, making the viscosity of the dispersion D become relatively higher.

3.5. Viscoelasticity and microscopy study of the starch dispersions

The rheological properties of starch dispersions were determined by its micro-structure, therefore, the viscoelasticity and microscopy studies of the samples could provide useful information about their rheological behaviors. The variation of G', G″, and tan δ as a function of angular frequency (ω) of the samples was given in Fig. 5.

It can be seen from Fig. 5 that G' curves of samples A–C decreased in sequence in relation to pasting extent of the WMS dispersions. As shown in Fig. 6, when the WMS dispersion was pasted more completely, its granules dissolved more effectively into the continuous phase, making the G' value smaller at the same angular frequency. Meanwhile, except for fluctuates at low frequencies for the dispersion A, G'' curves of dispersion A–C nearly overlapped with each other, indicating a very limited effect of pasting conditions on G'' for the WMS dispersions. The G' and G'' curves of the sample D were obviously higher than those of the WMS dispersions, which was ascribed to different micro-structures. As seen in Fig. 6(D), the NMS granules dissolved almost completely into the continuous phase. As indicated previously, amylose molecules leached out from granules during pasting have the capacity to form a network stabilized by hydrogen bonds, which could determine the formation of gel-type structures of the pastes upon cooling (Iturriage et al., 2006). During resting and testing at 25 °C, due to the formation of the gel-type structures, the dispersion D had larger G' and G''. For the WMS which was amylose free, the continuous phase is essentially amylopectin dissolved during swelling of the granules (Rodríguez-Hernández et al., 2006). Therefore, the dispersions of WMS cannot form gels under normal conditions (Banks & Greenwood, 1975). As a result of the different micro-structures of the WMS and NMS dispersions, these starch dispersions showed distinctly different rheological properties.

The dynamic rheological data of log (G', G'') vs. log ω were subjected to linear regression, and Table 2 gives the magnitudes of slopes (n' and n''), intercepts (K' and K''), and R^2 in Eqs. (2) and (3) (Özkan, Xin, & Chen, 2002):

$$G' = K'\omega^{n'} \quad (2)$$

$$G'' = K''\omega^{n''} \quad (3)$$

From Table 2, K' and K'' at a certain extent reflected the magnitudes of G' and G'', respectively. The n' value of the dispersion D was much smaller than other samples, indicating a less susceptibility of G' to the change of ω. The differences of n'' between the samples were relatively limited, indicating a similar susceptibility of G'' with ω for all samples. The tan δ (G''/G') values of the sample D increase with the increasing of ω, however, the opposite behavior was observed for the samples A–C.

4. Conclusions

The WMS dispersions (5.0 wt.%) displayed both thixotropy and anti-thixotropy in the loop and shear recovery tests depending on the pasting conditions. When the WMS dispersions were pasted

sufficiently, they showed anti-thixotropic behavior, which became more significant at higher temperatures. The standard anti-thixotropy test showed that the anti-thixotropy of WMS dispersions only appeared at certain shear rates. When pasted more completely, the anti-thixotropic behavior of the WMS dispersions was observed at higher shear rates and wider shear rate range, furthermore they displayed improved thermal stability. The viscoelasticity and microstructural studies indicated that the micro-structures of the WMS and NMS dispersions were different, which lead to different rheological properties. The anti-thixotropy of the WMS dispersions was ascribed to rearrangement of the amylopectin molecules under appropriate shear rates. The NMS dispersion (5.0 wt.%) could not display anti-thixotropy in this study, due to a different micro-structure formed by amylose in the continuous phase.

Acknowledgements

Supported by Program for New Century Excellent Talents in University of China (NCET-08-0537), National Natural Science Foundation of China (30800662), Science and Technology Research Key Program of China (105014), and Research and Development Fund for University's Doctoral Discipline of China (20050019029).

References

Achayuthakan, P., & Suphantharika, M. (2008). Pasting and rheological properties of waxy corn starch as affected by guar gum and xanthan gum. *Carbohydrate Polymers, 71*, 9–17.

Acquarone, V. M., & Rao, M. A. (2003). Influence of sucrose on the rheology and granule size of cross-linked waxy maize starch dispersions heated at two temperatures. *Carbohydrate Polymers, 51*, 451–458.

Banks, W., & Greenwood, C. T. (1975). *Starch and its components*. Edinburgh University Press. pp. 52.

Barnes, H. A. (1997). Thixotropy-a review. *Journal of Non-newtonian Fluid Mechanics, 70*, 1–33.

Bhandari, P. N., Singhal, R. S., & Kale, D. D. (2002). Effect of succinylation on the rheological profile of starch pastes. *Carbohydrate Polymers, 47*, 365–371.

Bird, R. B., & Marsh, B. D. (1968). Viscoelastic hysteresis. I. model predictions. *Transactions of the Society of Rheology, 12*, 479.

Blanshard, J. M. V. (1995). The glass transition, its nature and significance in food processing. In S. T. Beckett (Ed.), *Physico-chemical aspects of food processing* (pp. 17–48). Glasgow: Blackie and Academic Professional.

Chamberlain, E. K., Rao, M. A., & Cohen, C. (1999). Shear thinning and anti-thixotropic behavior of a heated cross-linked waxy maize starch dispersion. , 2, 63–77. *International Journal of Food Properties, 2*, 63–77. Errata, 2, 195–196.

Dewar, R., & Joyce, M. J. (2006). The thixotropic and rheopectic behavior of maize starch and maltodextrin thickeners used in dysphagia therapy. *Carbohydrate Polymers, 65*, 296–305.

Enes, P., Panserat, S., Kaushik, S., & Oliva-Teles, A. (2006). Effect of normal and waxy maize starch on growth, food utilization and hepatic glucose metabolism in European sea bass (*Dicentrarchus labrax*) juveniles. *Comparative Biochemistry and Physiology – A Molecular and Integrative Physiology, 143*, 89–96.

Ferguson, J., & Kembowski, Z. (1995). *Reologia Stosowana Pynów*. ódź: Wydawnictwo Marcus. pp. 42–47.

Gouveia, L. M., Muller, A. J., Marchal, P., & Choplin, L. (2008). Time effects on the rheological behavior of hydrophobically modified polyacrylamide aqueous solutions mixed with sodium dodecyl sulfate (SDS). *Colloids and Surfaces A: Physicochemical and Engineering Aspects, 330*, 168–175.

Hibi, Y. (2001). Effect of retrograded waxy corn starch on bread staling. *Starch/Stäerke, 53*, 227–234.

Iturriage, L. B., Mishima, B. L., & Anon, M. C. (2006). Effect of amylose on starch pastes viscoelasticity and cooked grains stickiness in rice from seven argentine genotypes. *Food Research International, 39*, 660–666.

Kim, S., Willett, J. L., Carriere, C. J., & Felker, F. C. (2002). Shear-thickening and shear-induced pattern formation in starch solutions. *Carbohydrate Polymers, 47*, 347–356.

Kim, W. W., & Yoo, B. (2009). Rheological behavior of acorn starch dispersions: Effects of concentration and temperature. *International Journal of Food Science and Technology, 44*, 503–509.

Kulicke, W. M., Eidam, D., Kath, F., Kix, M., & Kull, A. H. (1996). Hydrocolloids and rheology: Regulation of visco-elastic characteristics of waxy rice starch in mixtures with galactomannans. *Starch/Stäerke, 48*(3), 105–114.

Lehmann, A., Volkert, B., Fischer, S., Schrader, A., & Nerenz, H. (2008). Starch based thickening agents for personal care and surfactant systems. *Colloids and Surfaces A: Physicochemical and Engineering Aspects, 331*, 150–154.

Mewis, J., & Wagner, N. J. (2009). Thixotropy. *Advances in Colloid and Interface Science, 147–148*(C), 214–227.

Mezger, T. G. (2002). Rotational tests. In U. Zorll (Ed.), *The rheology handbook: For users of rotational and oscillatory rheometers* (pp. 55–68). Hannover: Vincentz Verlag.

Mohammadifar, M. A., Musavi, S. M., Kiumarsi, A., & Williams, P. A. (2006). Solution properties of targacanthin (water-soluble part of gum tragacanth exudates from *Astragalus gossypinus*). *International Journal of Biological Macromolecules, 38*, 31–39.

Nurul, I. M., Azemi, B. M. N. M., & Manan, D. M. A. (1999). Rheological behavior of sago (*Metroxylon sagu*) starch paste. *Food Chemistry, 64*, 501–505.

Özkan, N., Xin, H., & Chen, X. D. (2002). Application of a depth sensing indentation hardness test to evaluate the mechanical properties of food materials. *Journal of Food Science, 65*(5), 1814–1820.

Pongsawatmanit, R., Temsiripong, T., Ikeda, S., & Nishinari, K. (2006). Influence of tamarind seed xyloglucan on rheological properties and thermal stability of tapioca starch. *Journal of Food Engineering, 77*, 41–50.

Pongsawatmanit, R., Temsiripong, T., & Suwonsichon, T. (2007). Thermal and rheological properties of tapioca starch and xyloglucan mixtures in the presence of sucrose. *Food Research International, 40*, 239–248.

Rao, M. A. (1995). Rheological properties of fluid foods. In M. A. Rao & S. S. H. Rizvi (Eds.), *Engineering properties of foods* (pp. 1–54). New York: Marcel Dekker, Inc..

Rodríguez-Hernández, A. I., Durand, S., Garnier, C., Tecante, A., & Doublier, J. L. (2006). Rheology-structure properties of waxy maize starch–gellan mixtures. *Food Hydrocolloids, 20*, 1223–1230.

Sands, A. L., Leidy, H. J., Hamaker, B. R., Maguire, P., & Campbell, W. W. (2009). Consumption of the slow-digesting waxy maize starch leads to blunted plasma glucose and insulin response but does not influence energy expenditure or appetite in humans. *Nutrition Research, 29*, 383–390.

Tattiyakul, J., & Rao, M. A. (2000). Rheological behavior of cross-linked waxy maize starch dispersions during and after heating. *Carbohydrate Polymers, 43*, 215–222.

Wang, B., Li, D., Wang, L.-J., Chiu, Y. L., Chen, X. D., & Mao, Z.-H. (2008). Effect of high-pressure homogenization on the structure and thermal properties of maize starch. *Journal of Food Engineering, 87*, 436–444.

Wang, B., Wang, L.-J., Li, D., Özkan, N., Li, S.-J., & Mao, Z. H. (2009a). Rheological properties of waxy maize starch and xanthan gum mixtures in the presence of sucrose. *Carbohydrate Polymers, 77*, 472–481.

Wang, Y., Wang, L.-J., Li, D., Xue, J., & Mao, Z.-H. (2009b). Effects of drying methods on rheological properties of flaxseed gum. *Carbohydrate Polymers, 78*, 213–219.